


ORIGINAL RESEARCH

# Combining Optimized Image Processing With Dual Axis Rotational Angiography: Toward Low-Dose Invasive Coronary Angiography

Dimitri Buytaert , MSc; Benny Drieghe, MD; Frédéric Van Heuverswyn, MD; Jan De Pooter, MD, PhD; Peter Gheeraert, MD, PhD; Daniël De Wolf, MD, PhD; Yves Taeymans, MD, PhD; Klaus Bacher, PhD

**BACKGROUND:** Dual axis rotational coronary angiography (DARCA) reduces radiation exposure during coronary angiography on older x-ray systems. The purpose of the current study is to quantify patient and staff radiation exposure using DARCA on a modality already equipped with dose-reducing technology. Additionally, we assessed applicability of 1 dose area product to effective dose conversion factor for both DARCA and conventional coronary angiography (CCA) procedures.

**METHODS AND RESULTS:** Twenty patients were examined using DARCA and were compared with 20 age-, sex-, and body mass index-matched patients selected from a prior study using CCA on the same x-ray modality. All irradiation events are simulated using PCXMC (STUK, Finland) to determine organ and effective doses. Moreover, for DARCA each frame is simulated. Staff dose is measured using active personal dosimeters (DoseAware, Philips Healthcare, The Netherlands). With DARCA, median cumulative dose area product is reduced by 57% (ie, 7.41 versus 17.19 Gy·cm<sup>2</sup>). Effective dose conversion factors of CCA and DARCA are slightly different, yet this difference is not statistically significant. The occupational dose at physician's chest, leg, and collar level are reduced by 60%, 56%, and 16%, respectively, of which the first 2 reached statistical significance. Median effective dose is reduced from 4.75 mSv in CCA to 2.22 mSv in DARCA procedures, where the latter is further reduced to 1.79 mSv when excluding ventriculography.

**CONCLUSIONS:** During invasive coronary angiography, DARCA reduces radiation exposure even further toward low-dose values on a system already equipped with advanced image processing and noise reduction algorithms. For both DARCA and CCA procedures, using 1 effective dose conversion factor of 0.30 mSv·Gy<sup>-1</sup>·cm<sup>-2</sup> is feasible.

**Key Words:** cardiac catheterization ■ contrast media ■ coronary angiography ■ dual axis rotational angiography ■ effective dose ■ radiation dosing ■ rotational angiography

Coronary artery disease is an important cause of morbidity and mortality. Numbers of coronary angiographies (CA) and percutaneous coronary interventions (PCI) are still rising.<sup>1,2</sup> Diagnosis and treatment of coronary artery disease requires x-ray guidance during both CA and PCI. This may result in high radiation exposure levels for patients and staff, especially during complex interventions. Prevalence of lens

opacities in interventionalists is increasing, supporting the hypothesis of increased risk of cataract in occupationally exposed personnel.<sup>3–5</sup>

Projection angiograms in conventional coronary angiography (CCA) result in vessel overlap, vessel foreshortening, and unappreciated tortuosity.<sup>6–8</sup> Multiple studies report reduced radiation exposure during CA, using rotational angiography. The most recent type

Correspondence to: Dimitri Buytaert, MSc, Department of Human Structure and Repair, Ghent University, Proeftuinstraat 86, 9000 Ghent, Belgium. E-mail: dimitri.buytaert@ugent.be

Supplementary Material for this article is available at <https://www.ahajournals.org/doi/suppl/10.1161/JAHA.119.014683>

For Sources of Funding and Disclosures, see page 11.

© 2020 The Authors. Published on behalf of the American Heart Association, Inc., by Wiley. This is an open access article under the terms of the Creative Commons Attribution-NonCommercial License, which permits use, distribution and reproduction in any medium, provided the original work is properly cited and is not used for commercial purposes.

JAHA is available at: [www.ahajournals.org/journal/jaha](http://www.ahajournals.org/journal/jaha)

## CLINICAL PERSPECTIVE

### What Is New?

- While dual-axis rotational coronary angiography (DARCA) already proved useful on older systems, the current study assesses the impact of DARCA for invasive coronary angiography on a system equipped with dose-reducing technology that already demonstrated significant dose reductions in the recent past.
- Detailed estimation of organ and effective doses for each x-ray image frame of dual-axis coronary angiograms of the left and right coronary artery were conducted.
- Organ doses, effective dose, and dose area product-to-effective dose conversion factors have been established for DARCA procedures, and operator exposure is measured during DARCA procedures using real-time dosimeters.

### What Are the Clinical Implications?

- Also on x-ray modalities already equipped with dose-reducing technology, DARCA is able to significantly reduce radiation exposure for both patient and operator.
- Combining dose-reducing technology, in this case implemented as advanced image processing and additional copper filtration, with DARCA enables low-dose invasive coronary angiography.
- Provided that the x-ray energy spectrum of the conventional coronary angiography and DARCA protocols are comparable, the same dose area product-to-effective dose conversion factors can be used for DARCA as for conventional coronary angiography procedures.

### Nonstandard Abbreviations and Acronyms

<b>CA</b>	coronary angiography
<b>CAD</b>	coronary artery disease
<b>CCA</b>	conventional coronary angiography
<b>CF<sub>DAP-ED</sub></b>	dose area product to effective dose conversion factor
<b>CF<sub>DAP-OD</sub></b>	dose area product to organ dose conversion factor
<b>DAP</b>	dose area product
<b>DARCA</b>	dual-axis rotational coronary angiography
<b>ED</b>	effective dose
<b>LCA</b>	left coronary artery
<b>OD</b>	organ dose
<b>PCI</b>	percutaneous coronary intervention
<b>RCA</b>	right coronary artery

of rotational angiography is dual axis rotational coronary angiography (DARCA).<sup>9,10</sup> This technology shows high potential for dose reduction, both for patients and staff, since the coronary tree can be completely visualized using 2 rotations (ie, 1 for each coronary artery). Various studies show that DARCA reduces dose area product (DAP), air kerma, peak skin dose, scatter radiation, contrast volume consumption, and acute kidney injury when compared with CCA.<sup>11–19</sup>

The goal of the current study was to quantify the potential reduction in radiation exposure for both patients and staff during invasive CA, by using DARCA on a modality that is already equipped with dose-reducing technology. To our knowledge this is the first study to simulate organ doses (OD) and effective doses (ED) for both CCA and DARCA procedures in patients. Furthermore, this is the first study in which staff exposure is measured during clinical DARCA procedures instead of using phantom measurements.

## METHODS

The data that support the findings of this study are available from the corresponding author upon reasonable request.

### Study Population

Twenty consecutive adult patients, referred for clinically indicated diagnostic cardiac catheterization of the coronary arteries, were enrolled. CA for these 20 patients was performed using DARCA, and patient, operator, and staff radiation exposure levels were compared with 20 age, sex, and body mass index-matched patients selected from a prior study using CCA on the same equipment.<sup>20</sup> All 40 patients have thus been catheterized in the same catheterization laboratory. With matching, we aimed to equalize the age, sex, and body mass index distributions between both patient groups, yet cases were not individually matched.

Since the CCA procedures from the prior study were performed using femoral access, all DARCA procedures included in the current study were performed using femoral access, to prevent biasing the results by access site. Patients with coronary artery bypass grafting were excluded. In case of a combined diagnostic and interventional procedure, only data from the diagnostic part were retained for analysis and the PCI part was excluded from the current study. All patients gave their written informed consent to participate. The study protocol was approved by the Ethics Committee of Ghent University Hospital.

### Imaging Modality

All procedures (ie, all CCA and DARCA procedures) were performed in the same catheterization laboratory using the same x-ray modality (AlluraClarity FD20/10, Philips

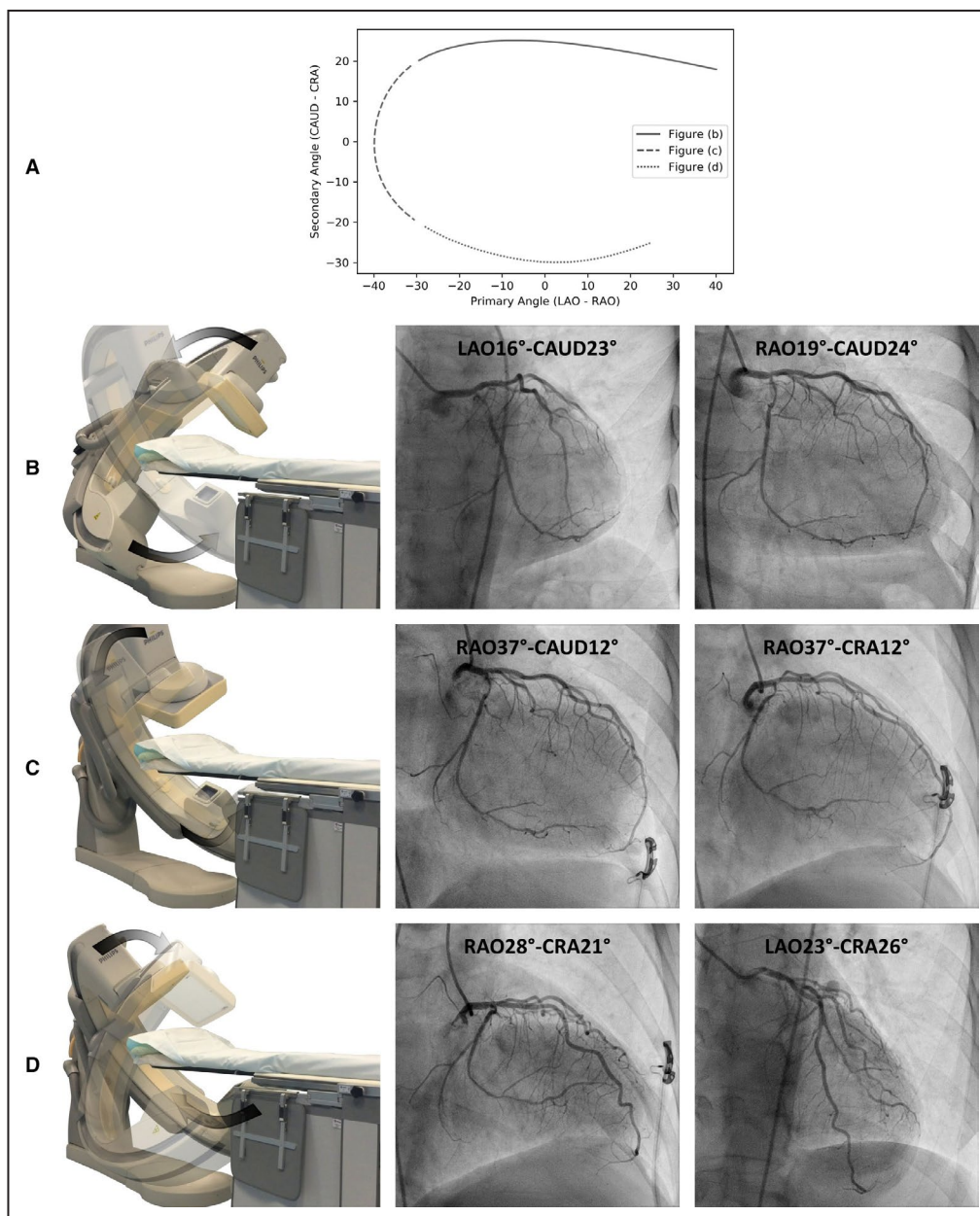


**Figure 1.** Graphical depiction of the C-arm movement during a DARCA acquisition of the left coronary artery.

The trajectory along which the C-arm moves during the acquisition is shown in (A). The acquisition starts at LAO40°-CAUD18° and can be split into 3 regions. Rows (B through D) each represent 1 region. For each region, the C-arm movement and a corresponding selection of 2 frames from an example DARCA angiogram are shown (B). The C-arm moves from an LAO to an RAO projection, while approximately maintaining the secondary projection angle constant in a caudal projection. C, Subsequently the C-arm is moved toward a cranial projection while keeping the primary angle roughly constant at an RAO projection and (D) eventually the C-arm travels back to an LAO projection while the secondary projection angle remains at an approximately constant cranial angle. Finally the acquisition ends at LAO25°-CRA25°. CAUD indicates caudal; CRA, cranial; DARCA, dual-axis rotational coronary angiography; LAO, left anterior oblique; and RAO, right anterior oblique.

Healthcare, Best, The Netherlands) equipped with both dose-reducing technology (ClarityIQ, Philips Healthcare, Best, The Netherlands) and DARCA technology (XperSwing, Philips Healthcare, Best, The Netherlands).

ClarityIQ combines powerful image processing, with optimized tube and detector settings to allow reduced dose settings without impairing clinical image quality.<sup>21</sup>

In CCA, multiple coronary angiograms for each coronary artery (left and right) are acquired at different projection angles to visualize the complete coronary tree. For each projection angiogram, the C-arm is first moved manually to one of the desired projections by an operator. Subsequently a contrast media injection and x-ray acquisition are initiated by the interventional cardiologist, during which the C-arm will remain stationary. In the CCA procedures, a standard acquisition protocol based on local practice was implemented, as described previously, including a lateral acquisition of both the left coronary artery (LCA) and right coronary artery (RCA) and a ventriculogram of the left ventricle.<sup>22</sup> DARCA allows for visualization of the whole coronary tree using merely 2 cinegraphy acquisitions, 1 for each coronary artery, during which the C-arm automatically follows a preprogrammed trajectory. This trajectory is designed by the manufacturer such that the C-arm passes by the projections most commonly acquired during CCA, including the optimal projections visualizing the major coronary segments with minimal vessel foreshortening and overlap,<sup>11</sup> in 1 continuous and automated movement and with a single contrast injection. Hence, the DARCA trajectory describes C-arm movement around both the left anterior oblique-right anterior oblique (LAO-RAO) and caudal-cranial (CAUD-CRA) axes simultaneously, as opposed to single-axis rotational angiography describing a circular motion within a single plane from LAO to RAO or vice versa while maintaining a constant orientation around the CAUD-CRA axis.<sup>9</sup> The DARCA trajectory for the LCA applied in this study is described in Figure 1 together with several frames of a resulting dual axis rotational coronary angiogram of the LCA. For the LCA, rotation starts at LAO40°-CAUD18° and ends at LAO25°-CRA25° after 5.3 s. A video of the C-arm trajectory together with an example of a resulting angiogram is given as an online data supplement (Video S1). Similarly as for the LCA, a preprogrammed DARCA trajectory was available for the RCA, starting at RAO30°-CAUD25° and stopping at LAO30°-CRA30° after 3.7 s. The standard acquisition protocol for DARCA was 1 DARCA acquisition for each coronary artery (1 left and 1 right) and a ventriculogram of the left ventricle.

The system powers up with the lowest dose settings as default. The cardiologists were requested to perform all procedures using these default settings. If necessary, cardiologists could acquire more projections and use higher dose settings. The lowest dose settings for the coronary protocols apply an additional beam filtration of 0.4 mm Cu+1 mm Al and a frame rate equal to 15 f/s in both the CCA protocols and the DARCA protocols. For the left ventricle protocol, 30 f/s is used with an additional 0.1 mm Cu+1 mm Al filtration. The tube has an inherent filtration of 2.5 mm Al and a tungsten anode at an 11° angle.

Contrast medium is administered using a contrast delivery system (ACIST CVI, Acist Medical Systems, Eden Prairie, MN). Contrast is automatically injected when x-ray acquisition is initiated. Selective DARCA angiograms of the LCA and RCA are acquired using a respective 2.1 and 1.2 mL/s contrast injection rate, and CCA angiograms apply 4 and 3 mL/s for the LCA and RCA respectively.

## Patient Exposure Evaluation

The catheterization laboratory is equipped with DICOM Radiation Dose Structured Reports, containing cumulative information about the patient's radiation exposure for the whole procedure, as well as information per irradiation event (ie, per fluoroscopy exposure and cinegraphy acquisition). At the end of each procedure, they are sent to a dose management system (DoseWatch, GE Healthcare, Milwaukee, WI).

For each procedure the average peak tube potential or kVp is calculated as the weighted sum of kVp values for all irradiation events, where the weighting factor per irradiation event is calculated as the corresponding DAP for said irradiation event divided by the cumulative DAP for that procedure. This is shown in formula (1):

$$kVp_{\text{procedure}} = \sum_i \left( \frac{DAP_i}{DAP_{\text{procedure}}} \right) kVp_i \quad (1)$$

where  $i$  is 1 irradiation event. Likewise, average additional filtration is calculated per procedure. With the latter parameters, aforementioned anode angle and inherent filtration as input, half value layer is then estimated using Spectrum Processor 3.0 for IPED report 78.<sup>23</sup>

## Patient Organ and Effective Doses

OD and ED are calculated using PCXMC, a Monte Carlo simulations software. The 40 procedures included in this study account for 1122 irradiation events, of which each is simulated automatically using PCXMC, in-house scripts, and a customized database. Dose area product to organ dose conversion factors from DAP to OD ( $CF_{\text{DAP-OD}}$ ) and dose area product to effective dose conversion factor ( $CF_{\text{DAP-ED}}$ ) are determined.

The DARCA acquisitions are considered a single irradiation event in the Radiation Dose Structured Reports, recording only the exposure parameters of the last frame. To calculate OD and ED of the DARCA acquisitions, the exposure parameters for each frame were estimated as follows. The manufacturer provided a look-up table demonstrating the automatic brightness and exposure control response on our modality. This look-up table contains the tube voltage, tube current, pulse width, and air kerma rate for each mm of Water Equivalent Thickness ranging from 150 to



400 mm Water Equivalent Thickness. A mathematical PCXMC phantom is selected based on patient age and adjusted to the patient's height and weight. Assuming that the heart is positioned at the isocenter of the C-arms, the patient thickness was calculated for each C-arm projection during the DARCA acquisition. From these thicknesses, the Water Equivalent Thickness was calculated by applying a single conversion factor, per DARCA acquisition, from phantom thickness to Water Equivalent Thickness. The latter conversion factor was numerically determined as the conversion factor that resulted in the minimal deviation of the air kerma for 1 DARCA acquisition obtained from the look-up table and the air kerma for the same DARCA acquisition obtained from the Radiation Dose Structured Reports. In total 5680 DARCA frames were simulated using PCXMC.

### Occupational Exposure Evaluation

Occupational dose was measured using the DoseAware Xtend system (Philips Healthcare, Best, The Netherlands). The latter system consists of a set of calibrated solid-state active personal dosimeters, logging the cumulative personal dose equivalent Hp(10) every second via a wireless base station. Hp(10) is an operational quantity for personal monitoring, defined as the dose equivalent to soft tissue at a depth of 10 mm below a specified point on the body (ie, the point where the dosimeter is worn). The latter parameter can be used to assess ED.<sup>24</sup> The characteristics of these dosimeters were described previously.<sup>25</sup> This system automatically sends staff dose data, in DICOM format, as an operator dose structured report, containing cumulative doses and mean dose rates per procedure, and per irradiation event, for each active personal dosimeter that was inside the catheterization laboratory during the procedure.

A set of 5 active personal dosimeters was used and worn above the lead apron. The physician's set contains 1 collar, and chest (breast pocket) and leg (left knee level) dosimeter. The technologists wore a collar and chest active personal dosimeter. The staff was blinded for their dosimeter readings.

### Statistical Analysis

For normally distributed variables, significance testing of differences between CCA and DARCA was performed using an independent samples *t* test with a 95% 2-sided CI. A Mann-Whitney test was performed in case of non-normality. Variables were summarized using median, 25<sup>th</sup> percentile (Q1), and 75<sup>th</sup> percentile (Q3). Comparison of categorical parameters was done using a  $\chi^2$  test for association, also applied with a 95% CI. All statistical analyses were performed using IBM SPSS Statistics 25 (IBM Corp, Armonk, NY).

**Table 1. Patient and Operator Exposure Data in DARCA and CCA Procedures**

	DARCA (n=20)	Conventional CA (n=20)	P Value
	Median (Q1–Q3)	Median (Q1–Q3)	
Demographic patient data			
Males/females	9/11	11/9	0.527
Age, y	71.5 (59.0–78.3)	68.0 (64.3–71.0)	0.975
BMI, kg/m²	26.6 (23.5–28.1)	27.8 (25.5–31.8)	0.079
Exposure parameters			
DAP total, Gy·cm²	7.41 (5.04–9.10)	17.19 (11.06–22.47)	<0.0005
DAP fluoro, Gy·cm²	3.17 (2.89–5.73)	3.95 (2.62–5.55)	0.495
DAP exposure, Gy·cm²	3.22 (2.38–5.00)	10.73 (8.73–16.45)	<0.0005
Air kerma, mGy	59.44 (45.52–79.69)	145.56 (100.23–184.81)	<0.0005
Cine runs, n	3.0 (3.0–4.0)	11.5 (10.3–12.0)	<0.0005
Exposure images, n	316 (278–385)	826 (749–913)	<0.0005
Fluoroscopy time, s	117 (93–158)	125 (100–147)	0.448
Fluoroscopy portion, %	51 (40–63)	26 (22–30)	<0.0005
CMC, mL	71 (63–81)	109 (99–121)	<0.001
Occupational dose (Hp10)			
Physician torso, µSv	20 (13–34)	50 (24–92)	0.007
Physician collar, µSv	21 (13–43)	25 (8–41)	0.841
Physician leg, µSv	42 (32–63)	97 (60–141)	0.004
Technician torso, µSv	2 (1–3)	3 (2–6)	0.068
Technician collar, µSv	2 (1–5)	2 (1–5)	0.738

Values are reported as median (Q1–Q3), where Q1 and Q3 are, respectively, the first and third quartiles. BMI indicates body mass index; CA, coronary angiography; CMC, contrast media consumption; DAP, dose area product; and DARCA, dual-axis rotational coronary angiography.

Correlation between DAP and OD and between DAP and ED was assessed using linear regression.  $CF_{DAP-OD}$  and  $CF_{DAP-ED}$  are determined as the slope coefficient of a linear regression analysis.

## RESULTS

### Patient Exposure Evaluation

An overview of patient radiation exposure is given in Table 1. Concerning patient demographics, no differences are noted. Regarding patient exposure, for all parameters except fluoroscopy DAP, fluoroscopy time, and  $CF_{DAP-ED}$ , statistically significant differences are observed. Total DAP and air kerma per procedure

are reduced by 57% ( $P<0.0005$ ) and 59% ( $P<0.0005$ ), respectively. Number of cinegraphy exposures and exposure images are, respectively, 74% ( $P<0.0005$ ) and 70% ( $P<0.0005$ ) lower for DARCA procedures compared with CCA examinations. Exposure DAP is 70% lower in DARCA procedures ( $P<0.0005$ ). Contrast media consumption is reduced by 35% when applying DARCA ( $P<0.001$ ). Although the use of higher dose settings was allowed when the default protocols did not suffice, only the default low-dose protocols were used in both the CCA and DARCA groups. Contrast media consumption amounts on average 7 and 6 mL for CCA projections of the LCA and RCA, respectively, and for DARCA the values are, respectively, 13 and 7 mL.

All procedures in this study include an acquisition of the left ventricle. When ventriculography is excluded, total DAP is equal to 5.46 (4.25–7.89) and 13.04 (9.59–18.49) Gy·cm<sup>2</sup> for DARCA and CCA procedures, respectively. Contribution of the left ventricle cinegraphy exposure to total DAP is equal to 16% in CCA procedures and 23% in DARCA procedures. Lateral acquisitions are known to result in high radiation exposure, are absent from both DARCA trajectories, and are therefore absent from DARCA procedures. Excluding both left ventricle and lateral acquisitions from the CCA procedures resulted in a DAP of 10.56 (8.16–15.69) Gy·cm<sup>2</sup>. After excluding the latter acquisitions, DAP in DARCA procedures is still significantly lower than in CCA procedures ( $P<0.0005$ ).

Average kVp and additional filtration is 87 kVp and 0.97 mm Al+0.34 mm Cu in CCA procedures and 85 kVp and 1.00 mm Al+0.34 mm Cu in DARCA procedures, resulting in a half value layer of 7.15 and 7.25 mm Al for the CCA and DARCA groups, respectively. The small differences in tube voltage ( $P=0.602$ ), additional Al filtration ( $P=0.512$ ), and Cu filtration ( $P=0.414$ ) were not statistically significant. This verifies that indeed the same dose settings were used in both groups, and that there was no significant difference in patient thickness between the CCA and DARCA groups.

Figure 2 shows the DARCA trajectories followed by the C-arm for both the LCA and RCA on top of a 2-dimensional histogram displaying the most used C-arm projections for cinegraphy during CCA.

As C-arm x-ray modalities are equipped with an automatic exposure control, the radiation output of the x-ray tube is adjusted continuously to keep the radiation dose rate at the detector level constant. With DARCA, the projection varies during the acquisition, meaning a different patient attenuation is encountered for each frame. Hence, DAP significantly varies during the acquisition, which is shown in Figure 3A and 3C for the DARCA protocol of the LCA and RCA, respectively.

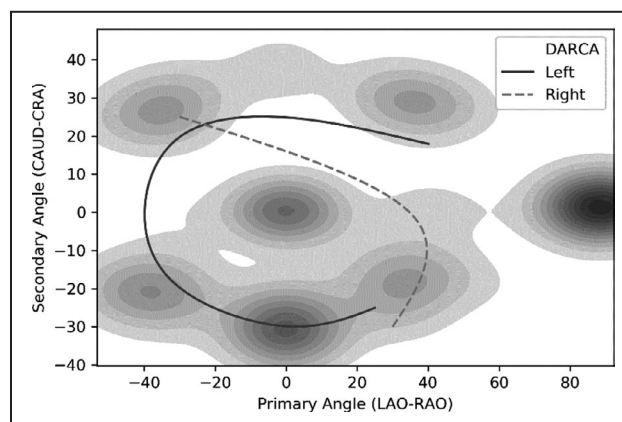


**Figure 2. Conventional projections and DARCA trajectories.**

The solid and dashed curves indicate the C-arm trajectory followed during DARCA acquisition of the LCA and RCA respectively. The shaded areas in the background show a 2-dimensional histogram of the cinegraphy projection angles used during CCA. Darker regions indicate more frequent projections. Projection angles within the white background are never applied. CAUD indicates caudal; CCA, conventional coronary angiography; CRA, cranial; DARCA, dual-axis rotational coronary angiography; LAO, cranial; LCA, left coronary artery; RAO, right anterior oblique; and RCA, right coronary artery.

## Patient Organ and Effective Doses

OD and ED are reported in Table 2. The table also displays between parentheses the average contribution of the organ to the total ED. Remainder organs include adrenals, extrathoracic airways, gallbladder, heart, kidneys, lymphatic nodes, muscle, oral mucosa, pancreas, prostate (male), small intestine, spleen, thymus, and uterus (female) according to International Commission on Radiological Protection publication 103. Although the heart is included in the remainder organs, heart OD was also assessed separately. OD in all organs is lower with DARCA compared with CCA. The lungs have the largest contribution to the total ED per procedure, accounting for on average 44% of total ED. When excluding the ventriculography at the end of the examination, ED further reduces to 4.18 (2.79–4.91) and 1.79 (1.46–2.84) mSv in the CCA and DARCA groups, respectively. When excluding the left ventricle and lateral acquisitions for CCA procedures, ED equals 3.34 (2.39–4.14) mSv, which remains a higher value than ED in DARCA procedures ( $P<0.0005$ ). DAP to OD ( $CF_{DAP-OD}$ ) and ED conversion factors ( $CF_{DAP-ED}$ ) are tabulated in Table 3.

Median (Q1–Q3) DAP for the left and right DARCA protocol is, respectively, equal to 0.84 (0.63–0.96) and 0.77 (0.60–0.90) Gy·cm<sup>2</sup>, ED for the left and right DARCA protocol is, respectively, equal to 0.36 (0.25–0.45) and 0.23 (0.20–0.27) mSv, and  $CF_{DAP-ED}$  for the left and right DARCA protocol is, respectively, equal to 0.29 (0.27–0.30) and 0.29 (0.27–0.32) mSv·Gy<sup>-1</sup>·cm<sup>-2</sup>.

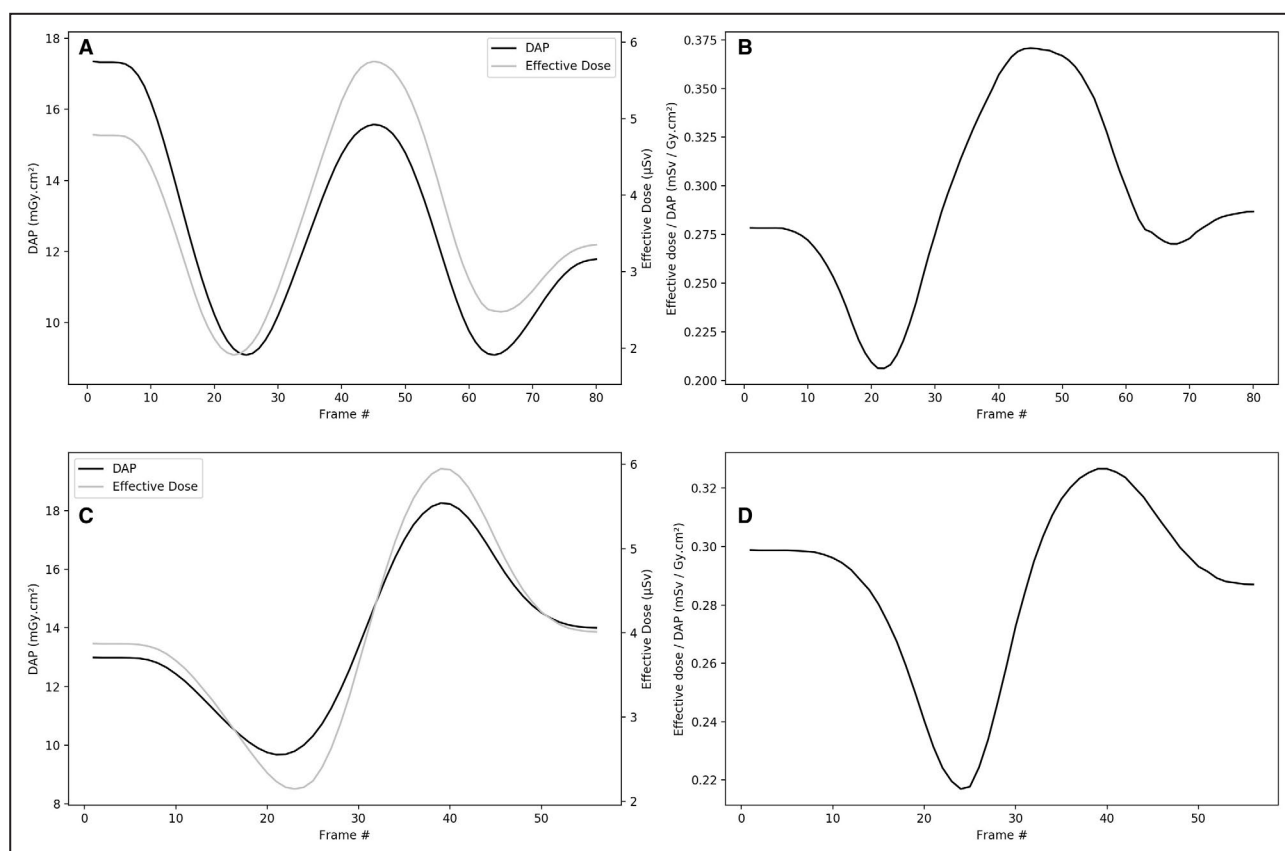


**Figure 3. Patient exposure per DARCA frame.**

**A**, DAP end ED per DARCA for the LCA. The left and right vertical axis show the respective DAP and ED ranges. **B**, Conversion factor from DAP to ED for each DARCA frame of the LCA. **C**, DAP and ED per DARCA frame for the RCA. The left and right vertical axis show the respective DAP and ED ranges. **D**, Conversion factor from DAP to ED for each DARCA frame of the RCA. ED indicates effective dose; DAP, dose area product; DARCA, dual-axis rotational coronary angiography; LCA, left coronary artery; and RCA, right coronary artery.

OD and consequently ED are directly proportional to the DAP. Therefore, ED varies accordingly for each frame along the trajectory, following a similar trend as the DAP. This is shown in Figure 3A and 3C. The frames with the largest ED are the 45th and 39th frame

of the left and right DARCA protocol, respectively, corresponding to RAO40°-CAUD0° and LAO40°-CRA9° C-arm projections. Additionally, the frames with the highest DAP do not necessarily yield the highest radiation detriment and risk; this is highly dependent on the

**Table 2. Organ and Effective Dose**

	DARCA (n=20)	CCA (n=20)	<i>P</i> Value
	Median (Q1–Q3)	Median (Q1–Q3)	
Organ doses, mGy			
Stomach (5.49%)	0.99 (0.8–1.44)	2.14 (1.59–2.76)	<0.0005
Liver (3.74%)	1.97 (1.36–3.23)	4.05 (2.81–5.93)	<0.0005
Lungs (44.26%)	7.37 (6.01–12.66)	17.49 (11.57–19.91)	<0.0005
Breasts (11.4%)	1.68 (1.23–3.4)	4.2 (3.1–4.47)	0.003
Esophagus (10.27%)	5.39 (4.57–8.21)	11.75 (8.79–14.55)	<0.0005
Remainder (9.94%)	1.74 (1.44–2.59)	4.34 (3.2–5.71)	<0.0005
Active bone marrow (12.31%)	2.31 (1.73–2.98)	4.86 (3.59–6.25)	<0.0005
Heart (3.22%)	7.28 (6.04–12.7)	15.78 (11.07–19.89)	<0.0005
Effective dose, mSv	2.22 (1.78–3.2)	4.75 (3.29–5.73)	<0.0005

Organ doses (mGy) of various organs and effective dose (mSv) in DARCA and CCA procedures. The average contribution of the organ's equivalent tissue dose to the total effective dose is displayed between parentheses. CCA indicates conventional coronary angiography; and DARCA, dual-axis rotational coronary angiography.

**Table 3.** CF<sub>DAP-OD</sub> and CF<sub>DAP-ED</sub>

	DARCA (n=20)	CCA (n=20)	<i>P</i> Value
	Slope (LL-UL)	Slope (LL-UL)	
CF <sub>DAP-OD</sub> , mGy/Gy·cm <sup>2</sup>			
Stomach	0.14* (0.13–0.15)	0.13* (0.12–0.14)	0.382
Liver	0.28* (0.22–0.34)	0.27* (0.23–0.31)	0.757
Lungs	1.11* (0.99–1.22)	0.99* (0.91–1.07)	0.135
Breasts	0.27* (0.19–0.35)	0.24* (0.19–0.3)	0.653
Esophagus	0.79* (0.74–0.83)	0.67* (0.63–0.72)	0.004
Remainder	0.25* (0.23–0.26)	0.26* (0.24–0.27)	0.478
Active bone marrow	0.31* (0.29–0.32)	0.29* (0.27–0.3)	0.074
Heart	1.12* (1.04–1.19)	0.93* (0.87–0.98)	0.001
CF <sub>DAP-ED</sub> , mSv/Gy·cm <sup>2</sup>	0.30* (0.27–0.33)	0.27* (0.25–0.29)	0.193

CCA indicates conventional coronary angiography; CF<sub>DAP-ED</sub>, DAP to effective dose conversion factor; CF<sub>DAP-OD</sub>, DAP to organ dose conversion factor; DAP, dose area product; DARCA, dual-axis rotational coronary angiography; LL, lower limit of the 95% CI; and UL, upper limit of the 95% CI.

\*Results of the linear regression analysis between DAP and either organ or effective doses. The slope coefficients are the conversion factors.

applied projection, yet the course of the CF<sub>DAP-ED</sub> variation during a DARCA acquisition describes a shape similar to that of DAP and ED. The frames with the highest ED also present the highest CF<sub>DAP-ED</sub>. This is displayed in Figure 3B and 3D.

## Occupational Exposure Evaluation

Occupational exposure is also summarized in Table 1. The physician's occupational dose is reduced by 60%, 16%, and 56% at chest, collar, and leg level,

respectively, in DARCA examinations. The difference at collar level, however, is not statistically significant. No statistically significant differences are observed for the technician's occupational dose.

## DISCUSSION

The results show that DARCA improved procedure safety by significantly reducing contrast media consumption and patient and operator radiation exposure compared with CCA. Since the same x-ray modality already demonstrated significant dose reduction by implementing noise reduction algorithms and additional filtration, introducing DARCA resulted in low-dose invasive CA procedures. Furthermore, we have shown that from DAP, displayed on most C-arm x-ray modalities, ED can be estimated using the same conversion factor for both DARCA and CCA procedures.

## Patient Exposure Evaluation

Patient exposure reduction can mainly be attributed to the reduced number of cinegraphy acquisitions (11.5 for CCA versus 3.0 for DARCA, ie, 74%). However, the number of exposure images is only 62% lower for DARCA procedures. The trajectories in Figure 2 imply complete absence of lateral acquisitions (LAO90°-CAUD0°) during DARCA procedures, while during CCA 1 lateral angiogram is acquired for each coronary artery. Lateral acquisitions result in higher DAP per frame. Hence, with 62% fewer exposure images in DARCA, a 70% lower exposure DAP still is reached.

Several studies compared CCA and DARCA in terms of DAP and contrast volume (Table 4).

**Table 4.** DAP and CMC in Literature Comparing CCA and DARCA

Reference	CCA		DARCA	
	DAP (Gy·cm <sup>2</sup> )	CMC (mL)	DAP (Gy·cm <sup>2</sup> )	CMC (mL)
Klein (2011) <sup>11</sup>	38.0±11.5	38.8±14.9	23.8±6.2	17.9±2.3
Grech (2012) <sup>12</sup>				
Monoplane	32.7±17.8	38.1±11.3	22.0±16.3	22.5±9.2
Biplane	56.7±28.6	27.8±10.8	30.9±18.5	24.4±7.7
Gomez-Mencherio (2012) <sup>13</sup>	27.6±11.5	93.1±41.7	18.0±6.4	50.9±14.7
Liu (2012) <sup>14</sup>	21.2±8.2	51.7±10.3	9.5±4.1	29.9±6.0
Yasar (2013) <sup>15</sup>	66.7±48.7	70.9±24.8	34.2±23.8	54.4±26.9
Farshid (2014) <sup>16</sup>	30.4±18.7	41.7±11.9	15.9±11.3	25.7±8.1
Giuberti (2014) <sup>17</sup>	30.0 (20.9–37.4)	76.0 (68.0–87.0)	20.0 (13.2–29.2)	60.0 (52.5–71.5)
Di Serafino (2018) <sup>18</sup>	...	80 (50–150)	...	40 (31–116)
Current study (2019)				
Including all acquisitions	17.2 (11.1–22.5)	109.3 (99.3–120.9)	7.4 (5.1–9.1)	71.0 (62.5–80.6)
Excluding left ventricle	13.0 (9.6–18.5)	79.3 (69.4–89.2)	5.5 (4.3–7.9)	43.7 (33.8–57.3)
Excluding left ventricle and lateral	10.6 (8.2–15.7)	66.3 (56.4–76.2)	5.5 (4.3–7.9)	43.7 (33.8–57.3)

CCA indicates conventional coronary angiography; CMC, contrast media consumption; DAP, dose area product; and DARCA, dual-axis rotational coronary angiography.



**Table 5. Number of Views During CCA of the LCA and RCA and Applied DARCA Protocols in Literature Comparing CCA and DARCA**

Reference	CCA No. Views		DARCA Irradiation Event Duration(s)	
	LCA	RCA	LCA	RCA
Klein (2011) <sup>11</sup>	4	2	6.7	4.0
Grech (2012) <sup>12</sup>				
Monoplane	5	2	5.3	3.7
Biplane	6 (=3×2)	2	5.3	3.7
Gomez-Menchero (2012) <sup>13</sup>	3	2	5.8	4.0
Liu (2012) <sup>14</sup>	5	2	5.8	4.0
Yasar (2013) <sup>15</sup>	4	2	...	...
Farshid (2014) <sup>16</sup>	4 to 5	2 to 3	5.8	3.7
Giuberti (2014) <sup>17</sup>	4	2 to 3	5.8	4.1
Di Serafino (2018) <sup>18</sup>	3 to 6	2	...	2 CCA views
Current study (2019)	6	3	5.3	3.7

CCA indicates conventional coronary angiography; DARCA, dual-axis rotational coronary angiography; LCA, left coronary artery; and RCA, right coronary artery.

Compared with literature referenced in Table 4, the lowest DAP values are observed in the current study for both CCA and DARCA procedures. This is because of the availability of ClarityIQ technology. The x-ray modalities from the references in Table 4 are not equipped with the latter technology. Also, all procedures in the current study were performed using femoral access, while 4 out of 8 literature references applied radial access.<sup>12–14,18</sup> Some studies report a small but statistically significant increase using the radial approach compared with femoral access.<sup>26</sup> When PCI was indicated after DARCA or CCA, PCI was allowed during the same procedure, but only the data from the diagnostic part of the procedure were registered and analyzed. DARCA was not applied during the PCI part and cannot be applied during PCI since stationary acquisitions are needed; however, it helps in selecting the optimal projection for PCI. Therefore, as far as we know, there have not been any reports in the literature of DARCA being applied during PCI procedures. Only 3 out of 20 DARCA and 1 out of 20 CCA procedures were followed by PCI in the same procedure, hence the effect of DARCA during the diagnostic part on the PCI part could not be examined. Gómez-Menchero et al assessed the impact of DARCA on combined diagnostic and therapeutic procedures and recorded a 29% contrast medium volume reduction without any statistically significant radiation dose reduction when compared with the conventional technique.<sup>13</sup>

Averaged over all previous publications (Table 4), DAP was reduced by 42% because of DARCA, while

in the current study DAP was reduced by 57%. The more pronounced reduction in DAP in our study can be explained by either a larger number of views acquired during CCA or slightly shorter DARCA acquisitions (Table 5).

On the contrary, contrast media consumption in the current study is higher than the previous studies. However, this can be attributed to the ventriculography at the end of each procedure, which consumes 30 mL of contrast media that was included in our study and not in previous studies mentioned in Tables 4 and 5. When excluding the acquisition of the left ventricle from the analysis, contrast volume is comparable with values found in the literature.

The current study achieves among the lowest patient exposures for invasive coronary angiography.<sup>27,28</sup> Kuon et al still observe significantly lower values, with both state-of-the-art flat detector and older image intensifier systems.<sup>29</sup> The latter study analyzed the impact of radiation-reducing strategies, implemented by 1 senior highly experienced interventionalist over a period of 15 years, starting at 33.8 Gy·cm<sup>2</sup> and ultimately accomplishing an impressive 0.6 Gy·cm<sup>2</sup> for CCA. Examples of such radiation-reducing strategies are focusing on essential acquisitions and beam-on time, avoiding steep angulations, reducing frame rate, reducing detector dose, etc. Because cardiac departments generally use multiple interventionalists and technologists with varying experience, as in the current study, the latter DAP values of Kuon et al do not resemble standard clinical practice. However, they can be used as realizable benchmarks for individual performance when identical x-ray exposure settings are used. In our department, baseline DAP with reference technology was 57.56 Gy·cm<sup>2</sup>, which was reduced by introducing technology with additional filtration and advanced noise reduction algorithms to a value of 20.45 Gy·cm<sup>2</sup> for CCA procedures and combined CCA+PCI procedures.<sup>20</sup> In the current study we only retained CCA procedures, hence the lower 17.19 Gy·cm<sup>2</sup> observed here, compared with the former 20.45 Gy·cm<sup>2</sup> on the same system. Introducing DARCA yields a DAP value of 7.41 Gy·cm<sup>2</sup>, ie, a 9.78 Gy·cm<sup>2</sup> (57%) reduction compared with CCA using the same equipment ( $P<0.0005$ ).

### Patient Organ and Effective Doses

In Table 3 the esophagus and heart exhibit a statistically different CF<sub>DAP-OD</sub> for CCA compared with DARCA. This might be attributed to a more uniform deposition of the dose in these organs during DARCA procedures. Respectively, the heart and esophagus are completely and almost completely exposed to the direct beam of all exposures. By using a limited

number of projections during CCA, the dose deposition might result in dose outliers within the volume of the directly exposed organs. This might have a different influence on the average organ dose than a continuous trajectory of projections as applied by DARCA, resulting in a more uniform dose distribution. Other organs are only partially exposed by the direct beam, resulting in nonuniform dose distributions for both CCA and DARCA procedures.

None of the references in Table 4 calculated OD and ED for CCA and DARCA. Several other studies provide either OD, ED,  $CF_{DAP-OD}$ ,  $CF_{DAP-ED}$ , or a combination of them obtained by Monte Carlo simulations using PCXMC for CCA and PCI procedures. Varghese et al reported mean DAP and ED values per projection for standard CCA procedures including 9 angiographic projections.<sup>30</sup> Summing DAP and ED over all projections results in 17.14 Gy·cm<sup>2</sup> and 4.93 mSv, respectively. Hence a  $CF_{DAP-ED}$  of 0.29 mSv·Gy<sup>-1</sup>·cm<sup>-2</sup> can be estimated from their study. Brambilla et al demonstrated an identical  $CF_{DAP-ED}$  as in the current study, (ie, 0.30 mSv·Gy<sup>-1</sup>·cm<sup>-2</sup>). They were also able to calculate OD and ED in CA and PCI procedures, taking into account all irradiation events. Only 2 isocenters were considered, 1 for male and 1 for female. This study adjusts the mathematical phantom dimensions and isocenter positions according to the patient's age and size, for each irradiation event, yielding a more accurate resemblance to reality. They note higher organ doses and similar  $CF_{DAP-OD}$  when compared with the current study because of their higher DAP and quite comparable  $CF_{DAP-OD}$ , except for the breasts.<sup>31</sup> Eloit et al simulated single-axis rotational angiography acquisitions in steps of 5°, evenly distributing DAP across the arc. Automatic brightness and exposure control was not taken into account. They observed a  $CF_{DAP-ED}$  of 0.183 mSv·Gy<sup>-1</sup>·cm<sup>-2</sup> for CCA procedures and a similar 0.179 mSv·Gy<sup>-1</sup>·cm<sup>-2</sup> for single axis rotational coronary angiography procedures. Likewise, in the current study  $CF_{DAP-ED}$  shows no statistically significant difference between CCA and DARCA examinations. Organ doses documented by Eloit et al are higher because of the higher DAP values in their study.<sup>22</sup>

To our knowledge only Wielandts et al, besides the current study, calculated OD and ED of rotational angiography on a per-frame basis accounting for the automatic brightness and exposure control. The latter study involved ablation procedures, with single-axis rotational angiography acquisition of the region (atria or left ventricle) of interest. Frame-specific information was available in their system's log files. No correlation was found between DAP and either OD or ED, hence no  $CF_{DAP-ED}$  could be determined. This was attributed to the limited tube output resulting in unexpected, almost body mass index independent, behavior of the automatic brightness and exposure control.<sup>32</sup>

## Occupational Exposure Evaluation

In 1 of our previous studies we tabulated Hp(10) values found in the literature.<sup>20</sup> Hp(10) values observed by Brasselet et al, Lo et al, and Tsapaki et al are still lower than the values in the current study for DARCA procedures; notwithstanding they documented higher DAP values.<sup>33–35</sup> This can be attributed to the use of additional radioprotective measures, such as ceiling suspended leaded glass, in the latter studies. Our current and previous studies did not apply such devices to prevent operator-dependent use of shielding and to inhibit collision of the C-arm with radioprotective tools during rotational angiography.

For the technician's exposure, no differences were observed between CCA and DARCA procedures. This might be attributed to the fact that they do not occupy a fixed position in the catheterization laboratory. They are continuously on the move. Since DARCA procedures need significantly fewer acquisitions, it seems reasonable that they spend relatively more time tableside while x-ray exposure is active during DARCA procedures than during CCA procedures, which eventually annihilates the effect of the DAP reduction on the technician's occupational exposure.

The physician's collar dosimeter recorded a smaller exposure reduction than the leg and chest dosimeter. Also here, movement of the dosimeter introduces higher uncertainty of the recorded dose because this is the most mobile of the 3 physician's dosimeters (ie, turning and/or tilting the head left or right results in significant change in position and orientation of the collar dosimeter). Since a dosimeter's position has a huge impact on the recorded dose, cf. the inverse square law, interpretation of the measured exposure is more reliable when including a recording of the dosimeter's position, which should be addressed in future research. Additionally, during CCA procedures the imaging detector is positioned as close as possible to the patient to minimize radiation exposure to the patient. This could block part of the scatter radiation to the collar dosimeter in posteroanterior, caudal, and right caudal projections (RAO≥0°-CAUD≥0°). Meanwhile, for DARCA acquisitions the source-to-imaging-detector distance is fixed at the largest distance (120 cm) to avoid collision with the patient, leaving a larger gap for the scatter radiation to reach the collar dosimeter. Furthermore, the caudal projections applied during CCA procedures are steeper compared with DARCA procedures.

## CONCLUSIONS

The x-ray modality used in this study has already demonstrated significant dose reduction when compared

with reference technology by implementing advanced image processing and noise reduction algorithms and adding extra filtration during fluoroscopy and cinegraphy exposures. Applying DARCA in invasive CA procedures reduces the dose even further toward low dose values. For both DARCA and CCA procedures,  $1 \text{ CF}_{\text{DAP-ED}}$  of  $0.30 \text{ mSv}\cdot\text{Gy}^{-1}\cdot\text{cm}^{-2}$  is appropriate and can be considered as a robust DAP to ED conversion factor for modern catheterization laboratories.

## ARTICLE INFORMATION

Received October 6, 2019; accepted April 24, 2020.

### Affiliations

From the Department of Human Structure and Repair, Ghent University, Ghent, Belgium (D.B., K.B.); Heart Center (B.D., F.V.H., J.D.P., P.G., Y.T.) and Department of Paediatric Cardiology (D.D.W.), Ghent University Hospital, Ghent, Belgium.

### Sources of Funding

This work is supported by the Agency for Innovation by Science and Technology (IWT, Flanders, Belgium), which is now part of Flanders Innovation and Entrepreneurship (VLAIO, Flanders, Belgium) (grant number 141670).

### Disclosures

None.

### Supplementary Material

Video S1

## REFERENCES

1. Eurostat. Health in the European Union—facts and figures. Available at: [https://ec.europa.eu/eurostat/statistics-explained/index.php/Health\\_in\\_the\\_European\\_Union\\_%E2%80%93\\_facts\\_and\\_figures](https://ec.europa.eu/eurostat/statistics-explained/index.php/Health_in_the_European_Union_%E2%80%93_facts_and_figures). Accessed May 17, 2019.
2. Benjamin EJ, Muntner P, Alonso A, Bittencourt MS, Callaway CW, Carson AP, Chamberlain AM, Chang AR, Cheng S, Das SR, et al.; on behalf of the American Heart Association Council on Epidemiology and Prevention Statistics Committee and Stroke Statistics Subcommittee. Heart disease and stroke statistics-2019 update: a report from the American Heart Association. *Circulation*. 2019;139:e56–e528.
3. Jacob S, Michel M, Spaulding C, Boveda S, Bar O, Brezin AP, Streho M, Maccia C, Scaiff P, Laurier D, et al. Occupational cataracts and lens opacities in interventional cardiology (O'CLOC study): are X-rays involved? Radiation-induced cataracts and lens opacities. *BMC Public Health*. 2010;10:537.
4. Shore RE. Radiation and cataract risk: impact of recent epidemiologic studies on ICRP judgments. *Mutat Res*. 2016;770:231–237.
5. Karatasakis A, Brilakis HS, Danek BA, Karacsonyi J, Martinez-Parachini JR, Nguyen-Trong PJ, Alame AJ, Roesle MK, Rangan BV, Rosenfield K, et al. Radiation-associated lens changes in the cardiac catheterization laboratory: results from the IC-CATARACT (cataracts attributed to radiation in the cath lab) study. *Catheter Cardiovasc Interv*. 2018;91:647–654.
6. Topol EJ, Nissen SE. Our preoccupation with coronary luminology. The dissociation between clinical and angiographic findings in ischemic heart disease. *Circulation*. 1995;92:2333–2342.
7. Scanlon PJ, Faxon DP, Audet AM, Carabello B, Dehmer GJ, Eagle KA, Legako RD, Leon DF, Murray JA, Nissen SE, et al. ACC/AHA guidelines for coronary angiography: executive summary and recommendations. A report of the American College of Cardiology/American Heart Association Task Force on Practice Guidelines (Committee on Coronary Angiography) developed in collaboration with the Society for Cardiac Angiography and Interventions. *Circulation*. 1999;99:2345–2357.
8. Jin ZG, Zhang ZQ, Jing LM, Wei YJ, Zhang J, Luo JP, Yang SL, Ma DX, Liu Y, Han W, et al. Correlation between dual-axis rotational coronary angiography and intravascular ultrasound in a coronary lesion assessment. *Int J Cardiovasc Imaging*. 2017;33:153–160.
9. Klein AJ, Garcia JA. Rotational coronary angiography. *Cardiol Clin*. 2009;27:395–405.
10. Loomba RS, Rios R, Buelow M, Eagam M, Aggarwal S, Arora RR. Comparison of contrast volume, radiation dose, fluoroscopy time, and procedure time in previously published studies of rotational versus conventional coronary angiography. *Am J Cardiol*. 2015;116:43–49.
11. Klein AJ, Garcia JA, Hudson PA, Kim MS, Messenger JC, Casserly IP, Wink O, Hattler B, Tsai TT, Chen SY, et al. Safety and efficacy of dual-axis rotational coronary angiography vs. standard coronary angiography. *Catheter Cardiovasc Interv*. 2011;77:820–827.
12. Grech M, Debono J, Xuereb RG, Fenech A, Grech V. A comparison between dual axis rotational coronary angiography and conventional coronary angiography. *Catheter Cardiovasc Interv*. 2012;80:576–580.
13. Gomez-Menchero AE, Diaz JF, Sanchez-Gonzalez C, Cardenal R, Sanghvi AB, Roa-Garrido J, Rodriguez-Lopez JL. Comparison of dual-axis rotational coronary angiography (XPERSWING) versus conventional technique in routine practice. *Rev Esp Cardiol (Engl Ed)*. 2012;65:434–439.
14. Liu HL, Jin ZG, Yang SL, Luo JP, Ma DX, Liu Y, Han W. Randomized study on the safety and efficacy of dual-axis rotational versus standard coronary angiography in the Chinese population. *Chin Med J (Engl)*. 2012;125:1016–1022.
15. Yasar AS, Perino AC, Dattilo PB, Casserly IP, Carroll JD, Messenger JC. Comparison of a safety strategy using transradial access and dual-axis rotational coronary angiography with transfemoral access and standard coronary angiography. *J Interv Cardiol*. 2013;26:524–529.
16. Farshid A, Chandrasekhar J, McLean D. Benefits of dual-axis rotational coronary angiography in routine clinical practice. *Heart Vessels*. 2014;29:199–205.
17. Giuberti RS, Caixeta A, Carvalho AC, Soares MM, Abreu-Silva EO, Pestana JO, Silva Junior HT, Vaz ML, Genereux P, Fernandes RW. A randomized trial comparing dual axis rotational versus conventional coronary angiography in a population with a high prevalence of coronary artery disease. *J Interv Cardiol*. 2014;27:456–464.
18. Di Serafino L, Turturo M, Lanzone S, Marano M, Scognamiglio G, Trimarco B, Cirillo P, Esposito G, D'Agostino C. Comparison of the effect of dual-axis rotational coronary angiography versus conventional coronary angiography on frequency of acute kidney injury, X-ray exposure time, and quantity of contrast medium injected. *Am J Cardiol*. 2018;121:1046–1050.
19. Liu H, Jin Z, Deng Y, Jing L. Dual-axis rotational coronary angiography can reduce peak skin dose and scattered dose: a phantom study. *J Appl Clin Med Phys*. 2014;15:4805.
20. Buytaert D, Eloit L, Mauti M, Drieghe B, Gheeraert P, Taeymans Y, Bacher K. Evaluation of patient and staff exposure with state of the art X-ray technology in cardiac catheterization: a randomized controlled trial. *J Interv Cardiol*. 2018;31:807–814.
21. Eloit L, Thierens H, Taeymans Y, Drieghe B, De Pooter J, Van Peteghem S, Buytaert D, Gijs T, Lapere R, Bacher K. Novel X-ray imaging technology enables significant patient dose reduction in interventional cardiology while maintaining diagnostic image quality. *Catheter Cardiovasc Interv*. 2015;86:E205–E212.
22. Eloit L, Bacher K, Steenbeke F, Drieghe B, Gheeraert P, Taeymans Y, Thierens H. Three-dimensional rotational X-ray acquisition technique is reducing patients' cancer risk in coronary angiography. *Catheter Cardiovasc Interv*. 2013;82:E419–E427.
23. Cranley K, Gilmore BJ, Fogarty GWA, Desponds L. Catalogue of diagnostic x-ray spectra and other data (IPeM Report 78). (Electronic version prepared by Sutton D). The Institution of Physics and Engineering in Medicine and Biology. 1997.
24. European Commission. Technical recommendations for monitoring individuals occupationally exposed to external radiation. European Commission, Radiation Protection 160. (EC: Luxembourg) 2009.
25. Chirioti S, Ginjaume M, Vano E, Sanchez R, Fernandez JM, Duch MA, Sempau J. Performance of several active personal dosimeters in interventional radiology and cardiology. *Radiat Meas*. 2011;46:1266–1270.
26. Sciahbasi A, Frigoli E, Sarandrea A, Rothenbuhler M, Calabro P, Lupi A, Tomassini F, Cortese B, Rigattieri S, Cerrato E, et al. Radiation exposure and vascular access in acute coronary syndromes: the RAD-Matrix trial. *J Am Coll Cardiol*. 2017;69:2530–2537.

27. Padovani R, Vano E, Trianni A, Bokou C, Bosmans H, Bor D, Jankowski J, Torbica P, Kepler K, Dowling A, et al. Reference levels at European level for cardiac interventional procedures. *Radiat Prot Dosimetry*. 2008;129:104–107.
28. Siiskonen T, Ciraj-Bjelac O, Dabin J, Diklic A, Domienik-Andrzejewska J, Farah J, Fernandez JM, Gallagher A, Hourdakos CJ, Jurkovic S, et al. Establishing the European diagnostic reference levels for interventional cardiology. *Phys Med*. 2018;54:42–48.
29. Kuon E, Felix SB, Weitmann K, Buchner I, Empen K. Long-term strategies support autonomy in radiation safety in invasive cardiology. *J Cardiol*. 2016;68:43–48.
30. Varghese A, Livingstone RS, Varghese L, Kumar P, Srinath SC, George OK, George PV. Radiation doses and estimated risk from angiographic projections during coronary angiography performed using novel flat detector. *J Appl Clin Med Phys*. 2016;17:433–441.
31. Brambilla M, Cannillo B, Matheoud R, Compagnone G, Rognoni A, Bongo AS, Carriero A. Conversion factors of effective and equivalent organ doses with the air kerma area product in patients undergoing coronary angiography and percutaneous coronary interventions. *Phys Med*. 2017;42:189–196.
32. Wielandts JY, Smans K, Ector J, De Buck S, Heidbuchel H, Bosmans H. Effective dose analysis of three-dimensional rotational angiography during catheter ablation procedures. *Phys Med Biol*. 2010;55:563–579.
33. Brasselet C, Blanpain T, Tassan-Mangina S, Deschildre A, Duval S, Vitry F, Gaillot-Petit N, Clement JP, Metz D. Comparison of operator radiation exposure with optimized radiation protection devices during coronary angiograms and ad hoc percutaneous coronary interventions by radial and femoral routes. *Eur Heart J*. 2008;29:63–70.
34. Lo TS, Ratib K, Chong AY, Bhatia G, Gunning M, Nolan J. Impact of access site selection and operator expertise on radiation exposure; a controlled prospective study. *Am Heart J*. 2012;164:455–461.
35. Tsapaki V, Kottou S, Patsilinos S, Voudris V, Cokkinos DV. Radiation dose measurements to the interventional cardiologist using an electronic personal dosimeter. *Radiat Prot Dosimetry*. 2004;112:245–249.